

UNIVERSITY OF LJUBLJANA
FACULTY OF MATHEMATICS AND PHYSICS
DEPARTMENT FOR PHYSICS

Miha Nemevšek

Conductance quantization and quantum Hall effect

Seminar

ADVISER: Professor Anton Ramšak

Ljubljana, 2004

Abstract

The purpose of this seminar is to present the phenomena of conductance quantization and of the quantum Hall effect. First, I will describe the experiment and comment on results. Then, I will present the theoretical background, which explains both phenomena by describing subband opening in a narrow constriction. Finally, I will focus on the latest breakthrough, that is imaging of electron flow through a constriction, confirming the theory.

Contents

| | | |
|----------|--|-----------|
| 1 | Introduction | 3 |
| 2 | The experiment | 3 |
| 3 | Theoretical background | 6 |
| 3.1 | Confined electrons ($U \neq 0$) in zero magnetic field ($B = 0$) | 7 |
| 3.2 | Free electrons ($U = 0$) in non-zero magnetic field ($B \neq 0$) | 8 |
| 3.3 | Confined electrons ($U \neq 0$) in an external magnetic field ($B \neq 0$) | 9 |
| 4 | Conductance quantization | 9 |
| 4.1 | Quantization | 10 |
| 4.2 | Energy averaging of the conductance | 12 |
| 5 | Quantum Hall effect | 12 |
| 6 | Imaging the electron flow | 14 |
| 7 | Conclusion | 15 |

1 Introduction

The latest development in technology offers a lot of technics to build smaller and smaller devices, even on the nanoscale. In such systems, classically defined quantities often do not obey the same classical laws they do in the macroscopic world and quantum mechanics steps in sooner or later. An example are the so-called quantum wires, which confine electrons in a long and narrow channel [1].

The purpose of this seminar is to present measurements of electrical and Hall conductance in a constriction, and present a simple theoretical explanation.

Electrons are confined in a 2-dimensional electron gas (2DEG) in a semiconductor heterostructure, and a gate is placed upon using lithography. In this way, we are dealing with quasi one dimensional problem, as the confined electrons can freely move only in one direction. Measured longitudinal conductivity is not linearly dependent on the gate width, as classical equations would tell, but is increased in very clear steps.

When we apply a perpendicular magnetic field, and measure the Hall conductivity in the transverse direction, steps are clearly visible also.

The latest development in this field and the final confirmation is the direct imaging of electron flow, using the newest tunneling microscopic techniques.

2 The experiment

The first experiment, which spurred the interest in measuring conductance quantization was made by von Klitzing [2]. His group measured the quantization of the Hall resistance of a degenerate electron gas in a MOSFET inversion layer. The reason why the first measurement of the quantization was performed in presence of a large magnetic field ($B \cong 15$ T) is probably because of the absence of backscattering, which was explained later by Buttiker [3] and which we will also discuss further on. The inset in figure 1 shows a top view of the device used in the experiment with a length $L = 400 \mu m$ and width of $W = 50 \mu m$. A constant magnetic field is applied perpendicular to the device. The graph shows the Hall voltage U_H and the probe potential drop U_{pp} . We can clearly see the plateaus in the U_H which is accompanied with a large drop of U_{pp} .

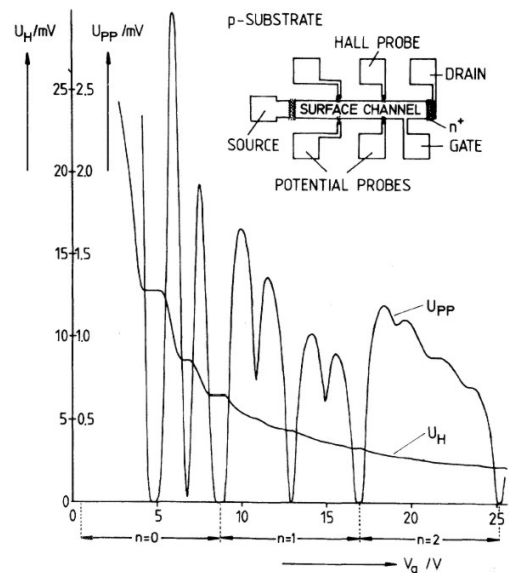


Figure 1: Recordings of the Hall voltage U_H and the voltage drop between potential probes U_{pp} at $T = 1.5$ K in a constant magnetic field $B = 18$ T and the source drain current $I = 1 \mu A$

This early experiment gave rise to many questions regarding the transport of electrons. However, as a result of a high mobility attained in a 2DEG trapped in a semiconductor heterostructure, the van Wees group [4] was able to measure the actual longitudinal conductance. The mean path of the electrons, due to their high mobility is actually significantly longer than the length of the constriction. Such constrictions are an ideal tool for studying ballistic transport of electrons and are called Sharvin point contacts. A classical description suffices, when the dimensions of the constriction are large compared to the electron Fermi wavelength λ_F , but when dimensions become comparable to λ_F the quantum ballistic regime is entered.

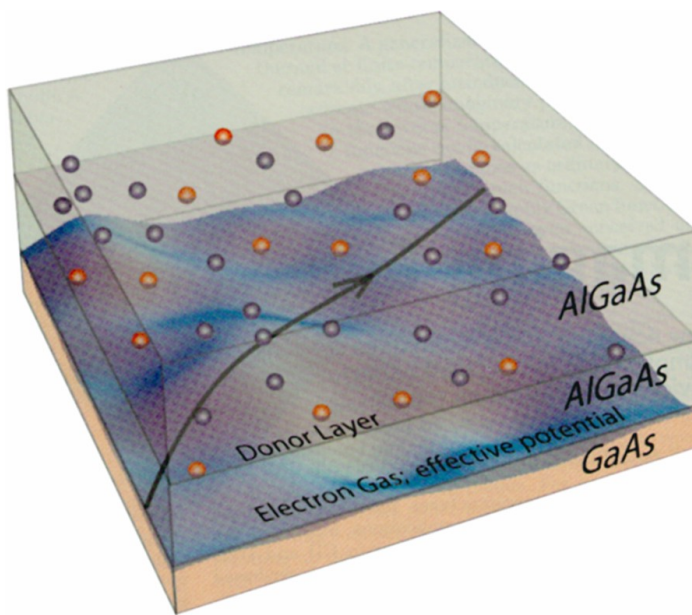


Figure 2: A 2DEG in a GaAs-AlGaAs heterostructure and the effective potential [5].

The point contacts are made on a high-mobility molecular-beam-epitaxy-grown GaAs-AlGaAs heterostructures, shown on figure 2. The electron density of the material is $3.56 \times 10^{15}/m^2$ and the mobility $85m^2/V s$ at 0.6 K. At such low temperatures both l_e and l_i can become relatively large ($10 \mu m$), as also λ_F which is typically 40 nm. Both conditions ($l_e \gg W$ and $\lambda_F \leq W$) were satisfied in the experiment described below.

The constriction was made on top of the heterostructure by creating a metal gate using electron-beam lithography (inset in Fig. 3). The geometric width of the gate was 250 nm, but the actual width is defined by applying gate voltage. At $V_g = 0.6V$, the electron gas beneath the gate is depleted, so the only way electrons can move is through the gate, not underneath. This is the maximum width. By reducing the voltage, the constriction is being tightened, so that when we reach $V_g = -2.2V$, the gate is fully shut and electrons cannot move through.

One would expect the conductance to increase linearly in respect to the width W of the constriction

$$G = \frac{2e^2}{h} k_F W / \pi, \quad (1)$$

but the conductance measurements shown in Fig. 3 show a striking difference. The dependance is not linear at all, as we can clearly see the plateaus at the integer multiples

of $2e^2/h$.

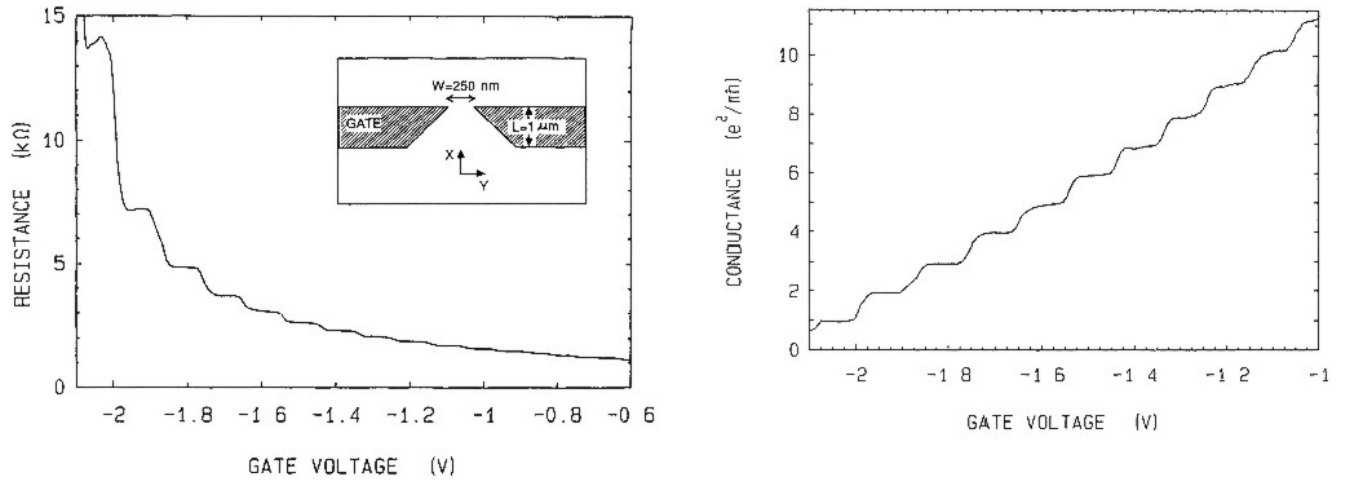


Figure 3: Left: Resistance of the point contacts as a function of gate voltage at 0.6 K. Inset: Point-contact layout. Right: Point-contact conductance obtained from resistance after subtraction of the lead resistance [4], [6].

We do not know though, how accurate the quantization is. In this particular experiment [6] the deviations from integer multiples of $2e^2/h$ might be caused by uncertainty in the resistance of the 2DEG leads.

In general, there are several factors, which determine the accuracy of quantization. This experiment was performed at 0.6 K. When we perform the experiment at higher temperatures, the effect decreases and we obtain an almost linear dependance at $T = 4.2$ K as seen if Fig. 4. The reason for this temperature averaging will be discussed later.

The other reason for deviations is the backscattering process. If we are dealing with a very "dirty" sample with a lot of impurities, we get a substantial decrease of conductance due to backscattering. The effect, however can be reduced by applying a strong magnetic field [3].

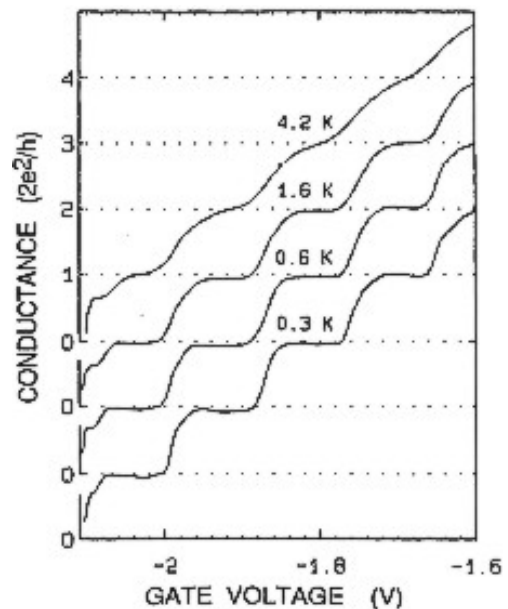


Figure 4: Breakdown of the quantization due to temperature averaging. The curves have been offset for clarity [6].

In an ideal material, the quantization is determined also by the shape of the constriction and especially by the potential. Such calculations have been done, considering sharp potential drop [7] and a smooth, saddle-like constriction [8].

A resumé of quantum ballistic and adiabatic electron transport was published by the van Wees group [6] and covers most of the measurements, including anomalous integer quantum Hall effect, which we will not discuss in this seminar.

3 Theoretical background

Now, we will discuss the theoretical background of the measurements we saw in the previous section. First, we will take a look at the description of transverse modes of an electron wavefunction in a narrow conductor, which is often referred to as an electron waveguide or a quantum wire. This is an introduction, but it is essential in many ways to understand the nature of the ballistic transport, especially in the presence of a large magnetic field.

Consider a long rectangular conductor that is uniform in x-direction and has some transverse confining potential $U(y)$ (see fig. 5).

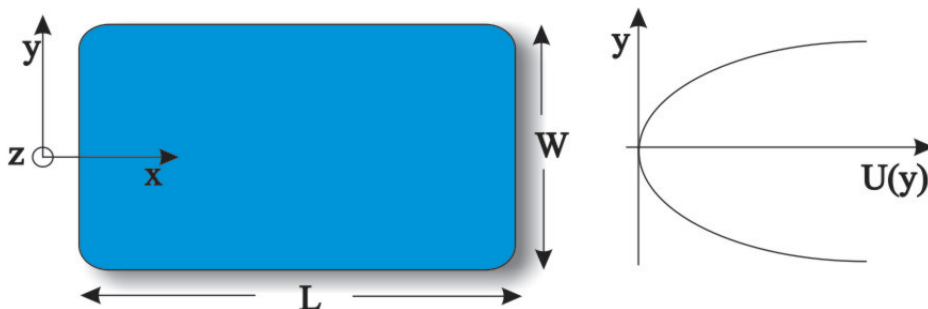


Figure 5: A rectangular conductor and a transverse confining potential.

We start with the general effective mass Schrödinger equation in an external magnetic field

$$\left[E_s + \frac{(i\hbar\nabla + e\mathbf{A})^2}{2m} + U(y) \right] \Psi(x, y) = E\Psi(x, y). \quad (2)$$

We apply a constant magnetic field B in a z direction, perpendicular to the x - y plane using the gauge

$$A_x = -By \quad \text{and} \quad A_y = 0. \quad (3)$$

The solution to Eq.2 can be expressed in the form of plane waves and a transverse function $\chi(y)$

$$\Psi(x, y) = \frac{1}{\sqrt{L}} \exp(ikx)\chi(y). \quad (4)$$

The transverse function $\chi(y)$ must satisfy the equation

$$\left[E_s + \frac{(\hbar k + eBy)^2}{2m} + \frac{p_y^2}{2m} + U(y) \right] \chi(y) = E\chi(y). \quad (5)$$

We have not yet defined confining potential $U(y)$. In general there are no analytical solutions for an arbitrary confining potential, therefore we have to make numerical calculations. However, analytical solutions are known for a potential well or a parabolic potential, which is a good description of the actual potential in many electron waveguides and which we will use in our discussion. We will consider confined electrons in three cases. First, we will compute the eigenenergies and eigenfunctions in the absence of the magnetic field ($B = 0$, $U \neq 0$), secondly the system with no potential, only magnetic confinement ($B \neq 0$, $U = 0$) and conclude with both, magnetic and potential confinement.

3.1 Confined electrons ($U \neq 0$) in zero magnetic field ($B = 0$)

In the case of zero magnetic field and parabolic potential

$$U(y) = \frac{1}{2}m\omega_0^2y^2, \quad (6)$$

Eq. 5 reduces to

$$\left[E_s + \frac{\hbar^2k^2}{2m} + \frac{p_y^2}{2m} + \frac{1}{2}m\omega_0^2y^2 \right] \chi(y) = E\chi(y). \quad (7)$$

This equation is equal to that of a harmonic oscillator with an energy shift of $E_s + \frac{\hbar^2k^2}{2m}$, and the eigensystem is given by

$$\chi_{n,k}(y) = u_n(q) \quad \text{where} \quad q = \sqrt{m\omega_0/\hbar}y, \quad (8)$$

where

$$u_n(q) = \exp(-q^2/2) H_n(q), \quad (9)$$

H_n being the n -th Hermite polynomial. The shifted eigenenergies are

$$E(n, k) = E_s + \frac{\hbar^2k^2}{2m} + (n + \frac{1}{2})\hbar\omega_0, \quad n = 0, 1, 2, \dots \quad (10)$$

The electron group velocity, which we will later need to compute electric current is proportional to the slope of the dispersion curve $E(k)$

$$v_g(n, k) = \frac{1}{\hbar} \frac{\partial E(n, k)}{\partial k}, \quad (11)$$

which is $\frac{\hbar k}{m}$ in our case.

States with different n -s are said to belong to different subbands. The energy spacing between subbands equals $\hbar\omega_0$ and the tighter the confinement the larger ω_0 and further

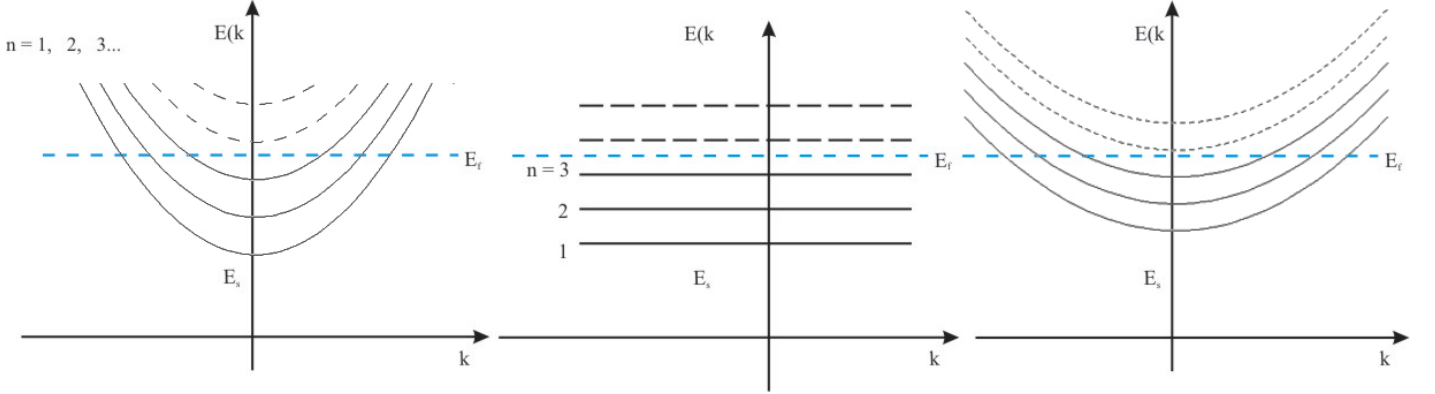


Figure 6: Comparison of the dispersion relation for the three aforementioned cases. **a)** $U \neq 0$ and $B = 0$, **b)** $U = 0$ and $B \neq 0$, **c)** $U \neq 0$ and $B \neq 0$.

apart the energy subbands. This mechanism is directly responsible for the steps observed in the conductance measurements in Fig.3. One is able to regulate the energy spacing $\hbar\omega_0$ by applying voltage between quantum point contacts.

3.2 Free electrons ($U = 0$) in non-zero magnetic field ($B \neq 0$)

In this case the Eq.(5) is reduced to

$$\left[E_s + \frac{(\hbar k + eBy)^2}{2m} + \frac{p_y^2}{2m} \right] \chi(y) = E\chi(y), \quad (12)$$

by defining $y_k = \hbar k / eB$ and $\omega_c = |e|B/m$ Eq.(12) is rewritten in the form

$$\left[E_s + \frac{p_y^2}{2m} + \frac{1}{2}m\omega_c^2(y + y_k) \right] \chi(y) = E\chi(y). \quad (13)$$

Eigenfunctions remain the same as in the previous case, the only difference is, they are centered around q_k instead of zero

$$\chi_{n,k}(y) = u_n(q + q_k) \quad \text{where} \quad q = \sqrt{m\omega_c/\hbar}y \quad q_k = \sqrt{m\omega_c/\hbar}y_k. \quad (14)$$

The mathematics describing these Landau levels i.e. magnetic subbands is thus very similar to the mathematics describing the electronic subbands for a parabolic confining potential. Physical content, however is completely different. Eigenenergies lose their k -dependence

$$E(n, k) = E_s + \left(n + \frac{1}{2}\right)\hbar\omega_c, \quad n = 0, 1, 2, \dots, \quad (15)$$

therefore their group velocity is 0! Although the eigenfunctions have the form of plane waves, a wave packet constructed of these localized states would not move. That is in accordance with classical dynamics, which predicts an orbital movement in an x - y plane.

The other important difference is that the eigenfunction offset y_k is proportional to the wave vector k in the longitudinal direction.

3.3 Confined electrons ($\mathbf{U} \neq \mathbf{0}$) in an external magnetic field ($\mathbf{B} \neq \mathbf{0}$)

Finally we consider the general case of confined electrons in an external magnetic field. We use the previously defined variables to convert Eq.(5) to a harmonic oscillator form

$$\left(E_s + \frac{p_y^2}{2m} + \frac{1}{2}m \frac{\omega_0^2 \omega_c^2}{\omega_{c0}^2} + \frac{1}{2}m\omega_{c0}^2 \left[y + \frac{\omega_c^2}{\omega_{c0}^2} y_k \right]^2 \right) \chi(y) = E\chi(y), \quad (16)$$

where

$$\omega_{c0}^2 = \omega_0^2 + \omega_c^2.$$

We can now easily write down the eigenfunctions and energies in the same manner we have done in the previous two cases

$$\chi_{n,k}(y) = u_n \left[q + q_k \right] \quad \text{where} \quad q = \sqrt{m\omega_{c0}/\hbar}y \quad q_k = \sqrt{m\omega_{c0}/\hbar}y_k, \quad (17)$$

$$E(n, k) = E_s + \left(n + \frac{1}{2} \right) \hbar\omega_{c0} + \frac{\hbar^2 k^2}{2m} \frac{\omega_0^2}{\omega_{c0}^2}, \quad n = 0, 1, 2, \dots \quad (18)$$

And the electron group velocity:

$$v_g(n, k) = \frac{1}{\hbar} \frac{\partial E(n, k)}{\partial k} = \frac{\hbar k}{m} \frac{\omega_0^2}{\omega_{c0}^2}. \quad (19)$$

Comparing the group velocity to $\hbar k/m$, it would seem that the effect of the magnetic field is the transformation of the effective mass,

$$m \rightarrow m \left[1 + \frac{\omega_0^2}{\omega_{c0}^2} \right]$$

which increases, as the magnetic field is increased.

If we compare the energy dispersion relations in Fig. 6, we see that the curves are stretched a little in the last case, when the magnetic field is increased. The number of levels below the Fermi energy depends on the gate width and/or the magnitude of the applied magnetic field.

4 Conductance quantization

In this section we will see, how to understand the plateaus measured in the experiment. First we will describe the conduction quantization in zero magnetic field, then we will discuss the effect of finite temperature and presence of a finite voltage in the samples.

Finally we will turn our attention to the effect of the magnetic field in a sample, and lay ground for understanding of the quantum Hall effect, which is the subject of the next section.

4.1 Quantization

Our task is to find an expression for conductivity, defined by a change of current, when voltage is applied

$$G = \frac{\delta I}{\delta U}. \quad (20)$$

We are familiar with the classical expression for the current density

$$dj = e v_g dn, \quad (21)$$

which is well defined for the case of free electrons, but we have to find the appropriate expression for each quantity in our case, when electrons flow through a potential barrier. First we have to be aware that each of the subbands contributes to the current, therefore we have to make a sum over all channels

$$dI = -eS \sum_m (dn_m v_{gm} \sum_n T_{mn}(E - V_0)). \quad (22)$$

It could quite possibly happen, that a wave function entering the constriction in a $n = 3$ transverse mode, would "split up", and leave the waveguide, say in 95% $n=3$ and 5% $n = 2$ mode. This is called channel mixing. To account for such phenomena, we define a transitivity matrix, which describes how the wave is transmitted. The matrix depends on the shape of the conductor and energy, we have also accounted for the shift of the potential in the constriction V_0 . To count all the contributions in the channel we use the inner sum over n in Eq. 22 and finally perform the outer sum over all m to get the complete current through a constriction.

The group velocity in the m channel is $v_{gm} = 1/\hbar dE_m/dk_m$ and the density of states in the volume unit is $2/Sdk_m/2\pi$, the 2 accounting for the two spin states. This would be true at very low temperatures, where all the electrons would be filled up to the Fermi energy. If the temperature is higher than 0 K, the states are filled up to the electrochemical potential μ and one has to multiply dn_m with the Fermi distribution function

$$f(E, T) = \frac{1}{e^{(E-\mu)/kT} + 1}. \quad (23)$$

Eq. 22 yields

$$dI = -\frac{2e}{h} T(E - V_0) f(E, T) dE. \quad (24)$$

This is the contribution to the current from one of the electrodes. If no voltage is applied, no current flows, since the contributions are the same. But when we apply the

voltage, electrons in one of the electrodes are filled to, say μ_L for the left and up to μ_R for the right electrode. The difference equals to $\delta\mu = e\delta U$, where δU is the applied voltage, see Fig.7.

Therefore, we have to subtract the contributions to get the net current, the result being

$$\delta I = -\frac{2e}{h} \int_{-\infty}^{\infty} T(E - V_0) (f(E - e\delta U, T) - f(E, T)) dE. \quad (25)$$

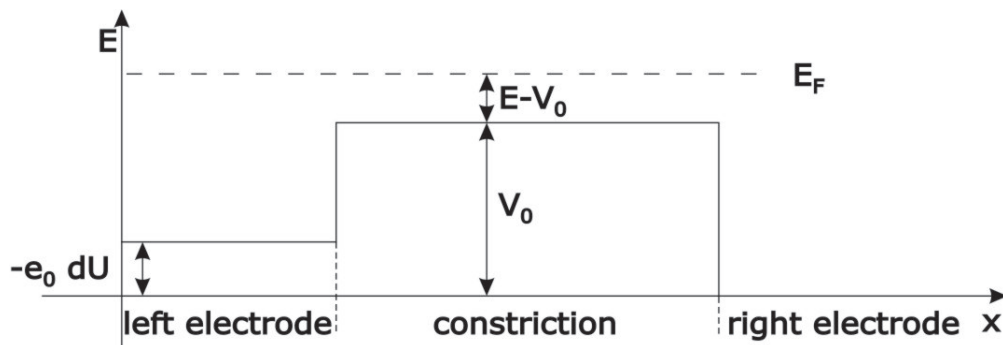


Figure 7: A sketch of the potential through the constriction.

When we use Eq. 20 and Eq.25, we get the final result

$$G(V_0, T) = \frac{2e^2}{h} \int_{-\infty}^{\infty} T(E - V_0) \left(-\frac{\partial f(E, T)}{\partial E}\right) dE. \quad (26)$$

If the potential is smooth there is no channel mixing, we get the adiabatic transport of the electrons and every electron is transmitted in the same state it is entered. If we idealize the case, all the current in each of the channels is transmitted completely, so that $T(E - V_0) = 1$.

In the low temperature ($T \rightarrow 0$) limit, all the electrons are filled up exactly to the Fermi energy and the Fermi distribution function is actually $\delta(E - E_F)$. Eq. 26 is simplified

$$G(V_0, T = 0K) = \frac{2e^2}{h} N(V_0), \quad (27)$$

where N is the number of the opened channels. This number depends on the gate voltage and can be inferred from the dispersion relation, e.g. from Eq. 18

$$N = \text{int} \left[\frac{E_F - eV_0}{\hbar\omega_{c0}} + \frac{1}{2} \right].$$

Now we can understand the origin of the quantization. The conductance is proportional to N , which is the number of opened channels. This number, however is defined by the number of subbands below the Fermi energy, see Fig. 6. When we tighten the constriction, either by applying gate voltage or increasing the magnetic field i.e. ω_0 or

ω_c , the energy gap increases, and the number of subbands with $E_n \leq E_F$ decreases. So, the tighter the constriction, the smaller the number of open channels, hence the smaller conductance. This is the fundamental mechanism behind both experiments, conductance quantization and integer quantum Hall effect.

4.2 Energy averaging of the conductance

We have also mentioned that quantization breaks down when temperature is increased, see Fig. 4. We can now understand this, if we take a look at Eq. 26. When performing the experiment a finite voltage V is applied across the device. In this case conductance is given by

$$G(V) = \frac{2e^2}{h} \frac{1}{V} \int_{E_F}^{E_F+eV} T(E - V_0) dE \quad (28)$$

Equations 26 and 28 show that in both cases, the physics is the same, only the weighing factors are different. The temperature averaging has a Gaussian weighing factor $(\partial f(E, T)/\partial E)$ which has an effective width $\Delta E \approx 4kT$, for voltage averaging $\Delta E = eV$. In the Fig. 8 transmission resonances are visible at $\Delta E < 0.45 \text{ meV}$ and disappear at higher ΔE . When temperature is further increased, the plateaus gradually disappear, see Fig. 3. The averaging becomes effective at 0.6 K and plateaus have almost disappeared at 4.2 K.

The mechanism for the destruction is that not all electron states are occupied at low-lying bands, some of the next subband is occupied also. This is why we put in the averaging factors that smooth the stepped curve.

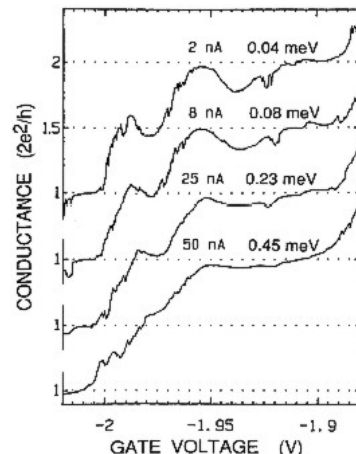


Figure 8: Voltage averaging of the resonances of G in the second subband.

5 Quantum Hall effect

In the previous section we have measured the longitudinal resistance of the 2DEG. Now, we will show that we can explain the quantization of the Hall resistance, which is measured in the perpendicular direction. First, we will take a look at the dispersion relation of the electrons in the 2DEG:

$$E_n(k_x) = eV(y) + (n - \frac{1}{2})\hbar\omega_c \pm g\mu_B B \quad (29)$$

We added the Zeeman splitting factor, which eliminates the spin degeneration and omitted other terms, which are small in the high field limit. As we have already mentioned,

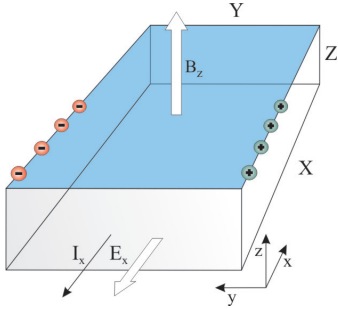


Figure 9: Classical Hall experiment

This is the setup of a classical experiment, which measures the Hall resistance. When a magnetic field is applied in the z direction and electrons travel in the x direction, the field moves the electrons to the left part of the sample as indicated in Fig. 9. The Hall voltage is defined by this field in the y direction: $U_H = E_y Y$. The Hall resistance is then calculated as $R_H = U_H / I_x$, where $I_x = nevYZ$ and n is the electron density and v the velocity (X , Y and Z are the sample dimensions). The velocity is obtained from equation: $eE_y = evB$, obtaining the final result : $R_H = B / Zne$

the eigenfunctions of the electrons are shifted along the y direction, depending on their group velocity. This means that the electrons coming from the left move on the upper part of the constriction and the ones coming from the left on the lower part. This is the mechanism that enables the formation of the edge channels.

The relevant electrons for transport are those at the Fermi energy and the electron in the n -th Landau level flows along the equipotential line defined by the condition

$$eV(y) = E_F - (n - \frac{1}{2})\hbar\omega_c \pm g\mu_B B \quad (30)$$

This condition is satisfied at the edges of the sample, so the edge channels are located at the intersection of the Landau levels and the Fermi energy as already indicated in Fig. 5. The sketch in Fig. 11 shows the occupied electron states in presence of a net current I in the 2DEG, which is a result of the difference in occupation of the right - and left-hand edge channels which carry the current in the opposite direction.

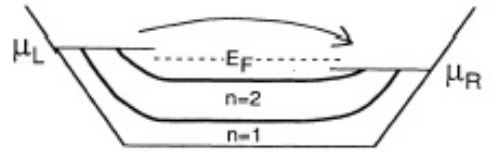


Figure 10: Cross section of a 2DEG showing the occupied electron states of two Landau levels in the presence of a current flow.

It can be shown that the net current I is independent of the details of the dispersion of the Landau levels and is given by

$$I = N_L \frac{e}{h} (\mu_L - \mu_R) \quad (31)$$

This is a direct consequence of Eq. 24 at low temperature when there is no need for a distribution function. Secondly, we measure the voltage in such a way we couple to all the opened channels, therefore the transmission coefficient is taken to be 1, which is true in a smooth potential where no channel mixing occurs.

The net current is given by the number of states in a Landau level multiplied by e/h and by the electrochemical potential difference $\mu_L - \mu_R$ between right and left edge

channels. Voltages probes attached to either side of the 2DEG will measure the potential difference, and the Hall resistance is

$$R_H = \frac{V_H}{I} = \frac{(\mu_L - \mu_R)}{eI} = \frac{h}{e^2} \frac{1}{N_L} \quad (32)$$

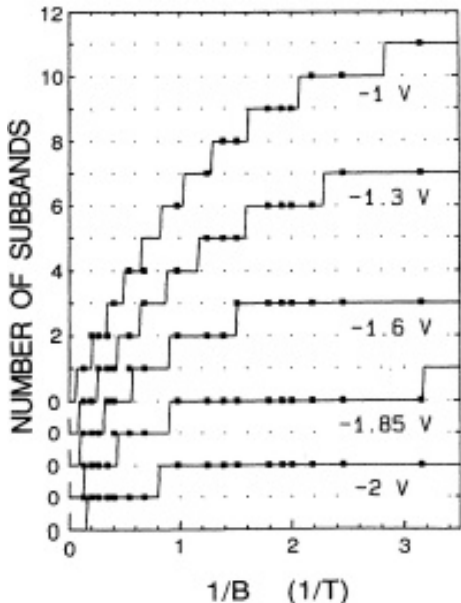


Figure 11: Number of subbands as a function of inverse magnetic field.

This is the simple explanation of the quantization of the Hall resistance. The number of subbands is proportional to $1/B$, so that the Hall resistance is proportional to B in accordance with the classical expression we derived earlier.

This is true for the currents in the bulk of the 2DEG. In the constriction, however, the number of occupied Landau levels is reduced relative to the bulk and is again given by the $N = \text{int}[(E_F - eV_0)/\hbar\omega_c + 1/2]$. The selective measurements of the channels, which does not couple to all subbands (as is the case in integer Hall effect), gives rise to a new phenomena called the anomalous integer quantum Hall effect, which we will not discuss here.

6 Imaging the electron flow

The latest breakthrough as already mentioned is the ability of imaging the electron flow directly during the experiments [5]. Imaging is performed on a 2DEG described above, as seen in Fig.2. Obtaining such images is not easy, because electrons are buried beneath the surface and because the sample must remain at a low temperature to show quantum behavior.

The Topinka group at Harvard used scanning probe microscopy to image the coherent flow of electron waves through the constriction, formed by the applied gate voltage (a in Fig.12).

This experiment was performed in absence of the magnetic field, or in presence of a small field. This is exactly the regime needed to obtain conductance quantization discussed above. They recorded the electron flow through the constriction and were able to measure each of the channel as the conductance increased in steps (b in Fig. 12). The inset shows the opening of the channels as the gate voltage is increased, as is the width of the constriction.

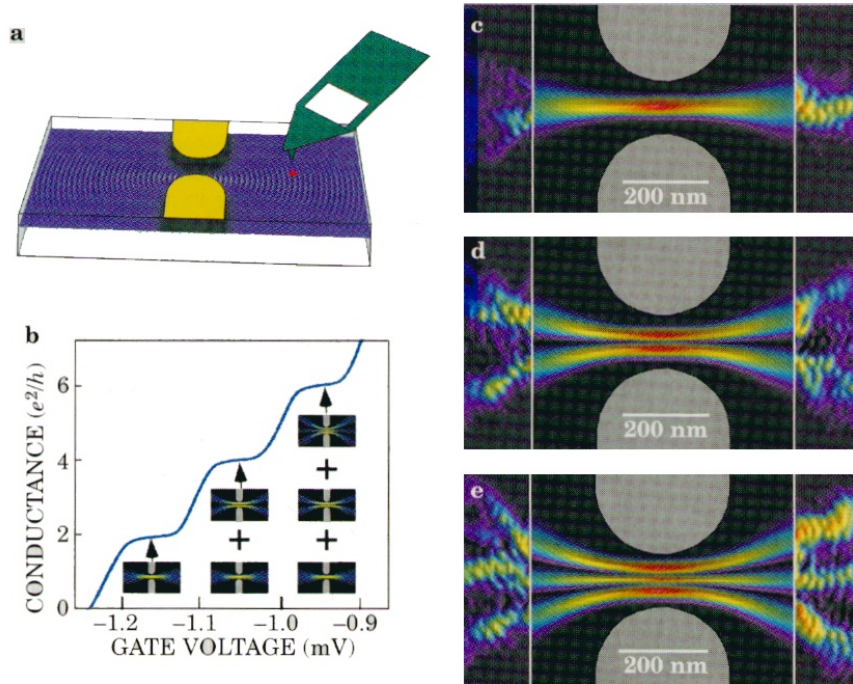


Figure 12: **a** Imaging the flow through QPC using a charged tip. **b** Conductance quantization

Results are represented in c, d and e in Fig. 12. The central part in the figure is a simulation, which is accompanied by the actual measurements on the edges. This is because we cannot measure the flow too near the constriction, as it would spoil the quantization due to the backscattering. We can see the modes with one, two and three maxima, as predicted by the calculated eigenfunctions of such a system. The ripples in the imaging figures are the electron waves with the Fermi wavelength λ_F .

7 Conclusion

We have shown the mechanism behind the phenomena of the quantized conduction and integer quantum Hall effect. We realized that the origin of the quantization lies in the opening of the subbands, the number of which is controlled either by applying the gate voltage and increasing ω_0 or by applying a perpendicular magnetic field.

We have seen that the quantization is obvious at low temperature and in the presence of a large magnetic field. The final confirmation is the imaging of the electron flow which shows the eigenfunctions of the confined electrons.

References

- [1] Reed Mark : Semiconductors and semimetals, vol.35 Nanostructured Systems, Yale University, New Haven, Connecticut, 1992
- [2] Klitzing K.v., Dorda G., Pepper M. : New Method for High-Accuracy Determination of the Fine-Structure Constant Based on Quantized Hall Resistance, *Phys. Rev. Lett.* **45** 494 (1980)
- [3] Buttiker M. : Absence of backscattering in the quantum Hall effect in multiprobe conductors, *Phys. Rev. B* **38** 9375 (1988)
- [4] van Wees B.J. et al., van Houten H. et al., Foxon C.T. : Quantized Conductance of Point Contacts in a Two-Dimensional Electron Gas, *Phys Rev Lett.*, **60** 848 (1988)
- [5] Topinka Mark A. : Imaging Electron Flow, *Physics Today* December 2003 p.47
- [6] van Wees B.J. et al., van Houten H. et al., Foxon C.T. : Quantum ballistic and adiabatic electron transport studied with quantum point contacts, *Phys Rev B*, **43** 12431 (1991)
- [7] Tekman E., Ciraci S. : Novel features of quantum conduction in a constriction, *Phys. Rev. B* **39** 8772 (1989)
- [8] Buttiker M. : Quantized transmission of a saddle-point constriction, *Phys. Rev. B* **41** 7906 (1990)
- [9] Žumer Slobodan, Kuščer Ivan : Toplota, Ljubljana 1987
- [10] Rejec Tomaž : Diplomaska naloga, Ljubljana, 1998
- [11] Strnad Janez : Fizika 3, Ljubljana 1998
- [12] Strnad Janez : Fizika 4, Ljubljana 1998